Decomposition filters for multi-exponential and related signals

Vairis Shtrauss

***Abstract*—**Decomposition of multi-exponential and related signals is generalized as a filtering problem on a logarithmic time or frequency scale and finite impulse response (FIR) filters operating with logarithmically sampled data are proposed to use for its implementation. The filter types and algorithms are found for various time-domain and frequency-domain mono-components. It is established that the ill-posedness of the multi-component decomposition manifests as high sampling-rate dependent noise amplification coefficients. A regularization method is proposed based on noise transformation control by choosing an optimum sampling rate. Algorithm design is suggested integrating together the signal acquisition, the regularization and the discrete-time filter implementation. As an example, the decomposition of a frequency-domain multi-component signal is considered by a designed discrete-time filter.

***Keywords*—**Decomposition, Distribution of time constants, Ill-posedness, Multi-component signals, Regularization**.**

I. Introduction

Many areas of science and technology, such as material science, mechanics, biology, nuclear and electrical engineering, etc. face the problem of analysing various monotonic or locally monotonic signals. The multi-component signals with the real decaying exponentials are probably the most studied case, although the similar problems arise also for many other monotonic mono-components, such as integrals, derivatives, real and imaginary parts of the Fourier transforms of the real exponentials, etc.

Although the problem of analysis of monotonic signals is not novel, let remember the works [1]–[6] became already the classical ones, the problem remains a challenging task for data processing. The principal reasons are the exceedingly non-orthogonal behaviour of the monotonic signals no constituting an orthogonal base, and the fundamental ill-posedness in the sense that small perturbations in input signal can yield unrealistic high perturbations in the results of decomposition.

Motivation of this work was to employ new possibilities coming from the novel data processing technologies and to develop accurate, robust and computationally efficient algorithms for analysing multi-component monotonic signals.

Manuscript received March 4, 2007; This work was supported by the Latvian Council of Science under Grant 05.1433. Revised received June 1,2007

V. Shtrauss is with the Institute of Polymer Mechanics of the University of Latvia, 23 Aizkraukles Street, Riga LV 1006 Latvia (corresponding author to provide phone: +371-675-43300; fax: +371-678-0467; e-mail: strauss@edi.lv).

II. Monotonic Multi-component Signals

Multi-exponential decays may be described by the following model

$$x(t)=\int_0^\infty G(\tau)\exp(-t/\tau)d\tau, \tag{1}$$

where $G(\tau)$ is a function of distribution of time constants (DTC) or spectrum of time constants. For the discrete (line) spectrum, $G(\tau)$ takes the form

$$G(\tau)=\sum_n G_n\delta(\tau-\tau_n),$$

where $\delta(\tau)$ is the Dirac delta function.

In some fields, e.g. in relaxation studies [7]–[9], model (1) is modified in the form

$$x(t)=\int_0^\infty F(\tau)\exp(-t/\tau)d\tau/\tau, \tag{2}$$

where new, so-called logarithmic DTC function $F(\tau)=G(\tau)\tau$, is introduced.

To generalize model (2) for other monotonic and locally monotonic signals, we modify it into the form

$$x(u)=\int_0^\infty F(\tau)K(u,\tau)d\tau/\tau, \tag{3}$$

where variable u is time or frequency, and kernel $K(u,\tau)$ represents a family of the time-domain and frequency-domain mono-components being of great importance in various fields

$$K(u,\tau)=\begin{cases}\exp(-u/\tau) & \text{(a)}\\ \exp(-u/\tau)/\tau & \text{(b)}\\ 1-\exp(-u/\tau). & \text{(c)}\\ 1/(1+u^2\tau^2 & \text{(d)}\\ u\tau/(1+u^2\tau^2 & \text{(e)}\\ u^2\tau^2/(1+u^2\tau^2 & \text{(f)}\end{cases} \tag{4}$$

Kernel (4a) is the basic real decaying exponential, whereas (4b) and (4c) represents its derivative and integral, respectively. In its turn, kernels (4d) and (4e) embodies the real and imaginary parts of the Fourier transform of kernel (4b). A pair of kernels (4f) and (4e) describes the frequency response of the system inverse to that characterized by a pair of kernels (4d) and (4e).

III. Filtering Approach for Decomposition

A. Background

Since kernels (4a) – (4f) depend on the ratio or product of arguments u and τ, multi-component signal (3) may be converted in the form of the Mellin convolution type transform

$$x(u) = F \overset{M}{*} k = \int_0^\infty F(\tau)k(u/\tau)d\tau/\tau\,, \tag{5}$$

where $\overset{M}{*}$ denotes the Mellin convolution and $k(u/\tau)$ represents kernels (4a) – (4f) modified in the form needed for converting (3) into (5).

The monotonic multi-component signals extend typically over long intervals of time or broad ranges of frequency [7]–[9], which is a reason for considering them on a logarithmic scale

$$u^* = \log_q u/u_0, \tag{6}$$

where u_0 is an arbitrary normalization constant. For logarithmic arguments (6), to remember that $u = u_0 q^{u^*}$, multi-component signal (5) alters into the appropriate Fourier convolution type transform ($u_0 = 1$)

$$x(q^{u^*}) = F(q^{u^*}) \overset{F}{*} k(q^{u^*}).$$

Consequently, DTC may be formally determined by the appropriate deconvolution

$$F(q^{u^*}) = x(q^{u^*}) \overset{F}{*} k^{-1}(q^{u^*}), \tag{7}$$

where $k^{-1}(q^{u^*})$ is inverse kernel existing in the sense of a generalized function.

In the frequency domain, deconvolution (7) may be described as

$$F_T(j\mu) = X(j\mu)/K(j\mu), \tag{8}$$

where $F_T(j\mu)$, $X(j\mu)$ and $K(j\mu)$ represent the Fourier transforms of functions $F(q^{u^*})$, $x(q^{u^*})$ and $k(q^{u^*})$ with logarithmically transformed arguments. At the same time, $F_T(j\mu)$, $X(j\mu)$ and $K(j\mu)$ may be expressed as the Mellin transforms of functions $F(u)$, $x(u)$ and $k(u)$ on linear scale. Here, parameter μ named further the 'Mellin frequency' can be interpreted as the frequency of a signal (function), whose independent variable (time or frequency) is logarithmically transformed.

Spectral representation (8) is a basis of the methods [1]–[4] implementing the decomposition according to the following general scheme

$$F(\tau) = \mathrm{IDFT}\{\mathrm{DFT}[x(q^{u^*})]/\mathrm{DFT}[k(q^{u^*})]\}, \tag{9}$$

where DFT and IDFT denote direct and inverse discrete Fourier transform, respectively. Similarly, spectral representation (8) is used also in the method [5], [6] implementing the decomposition by the direct and inverse discrete Mellin transforms ((DMT) and (IDMT))

$$F(\tau) = \mathrm{IDMT}\{\mathrm{DMT}[x(u)]/\mathrm{DMT}[k(u)]\}. \tag{10}$$

On the other hand, deconvolution (7) represents a *linear shift-invariant system* [10] or an *ideal decomposition filter on a logarithmic scale* having impulse response $k^{-1}(q^{u^*})$. The analytic expressions of $k^{-1}(q^{u^*})$ for kernels (4a) – (4f) are not known, however one may derive the appropriate frequency responses as the reciprocal of spectral function $K(j\mu)$, e.g. as the reciprocal of the Mellin transform of kernel $k(u)$

$$H(j\mu) = 1/M[k(u); -j\mu] = 1/\int_0^\infty k(u)u^{-j\mu-1}du\,. \tag{11}$$

Our idea is to implement deconvolution (7) in direct way by a finite impulse response (FIR) filter operating with equally spaced samples on a logarithmic scale

$$F(u_m^*) = \sum_{n=-\infty}^{\infty} h[n]x(u_{m-n}^*)\,, \tag{12}$$

where $h[n]$ is impulse response, which, of course, must be limited to the finite length in practice.

To take into consideration that equally spaced samples on a logarithmic scale creates the *logarithmic sampling* [11] with exponentially (according to the geometric progression) spaced data on linear scale

$$u_m = u_0\, q^m, \quad m = 0, \pm 1, \pm 2, \ldots,$$

algorithm (12) modifies into the following general form [11]-[13]:

$$F(u_0 q^m) = \sum_{n=-\infty}^{\infty} h[n]x\left(u_0 q^{m-n}\right). \tag{13a}$$

Here, progression ratio q specifies the sampling in the sense that ln$q$ plays a role of sampling period on a logarithmic scale.

Direct implementation of the decomposition by discrete-time filters has some advantages. First, its realization with hardware or software is much simpler, especially to take into consideration that the filter lengths are typically short (usually shorter than 10) due to the logarithmic sampling. Second, due to special algorithm design combined with the regularization [14] the direct implementation can potentially give the higher accuracy because does not require to perform the Fourier or Mellin transforms of the noisy and limited signals contributing the basic errors in approaches (9) and (10).

Conventional discrete-time filters (with the uniform sampling) [10] are used primarily for removing unwanted parts of a signal, such as random noise, or extracting useful parts of a signal, such as the components lying within a certain frequency range. Here, the discrete-time filters (with the logarithmic sampling) are proposed to use for performing functional transformation of signals to carry out decomposition (3). This new application requires the design and application philosophy [11]-[13], which differs from that of conventional discrete-time filters.

B. Algorithms of Decomposition Filters

Equation (3) with kernels (4a) and (4c) represents exactly the Mellin convolution type transform (5), for which algorithm (13a) can be directly applied to. For kernel (4b), general algorithm (13a) modifies into the form [11], [13]

$$F(u_0q^m) = u_0q^m \sum_{n=-\infty}^{\infty} h[n]x(u_0q^{m-n}), \quad (13b)$$

whereas for kernels (4d) – (4f), i.e. for the frequency-domain data, it modifies into the form

$$F(u_0q^m) = \sum_{n=-\infty}^{\infty} h[n]x(q^{-m-n}/u_0). \quad (13c)$$

Usually the considered here filters are used with the equal number of coefficients about the origin of the impulse response. Then, for odd number of filter coefficients N, general algorithm (13a) takes the form

$$F(u_0q^m) = \sum_{n=-(N-1)/2}^{(N-1)/2} h[n]x\left(u_0q^{m-n}\right), \quad (13d)$$

where the origin of the impulse response coincides with zero sample $h[0]$. For even number of filter coefficients, the origin may be located in the middle between the samples $h[-1]$ and $h[0]$, then algorithm (13a) modifies into the form

$$F(u_0q^m) = \sum_{n=-(N-2)/2-1}^{(N-2)/2} h[n]x\left(u_0q^{m-0.5-n}\right). \quad (13e)$$

C. Types of Decomposition Filters

For six kernels (4a) – (4f), reciprocals (11) give the three following ideal frequency responses

$$H(j\mu) = \begin{cases} -1/\Gamma(-j\mu) & \text{for (4a) - (4c)} \quad \text{(a)} \\ \pm \text{j2sh}(\pi\mu) & \text{for (4d) and (4f)} \quad \text{(b)} \\ 2\text{ch}(\pi\mu) & \text{for (4c)} \quad \text{(c)} \end{cases} \quad (14)$$

where (14a) relates to the time-domain data, (14b) – to the real parts, and (14c) – to the imaginary parts of the frequency-domain data, respectively. Consequently, only three independent sets of coefficients $h[n]$ are necessary for implementing decomposition (3) for six kernels (4a) – (4f). These filters have similar – very steep growing magnitude responses (Fig. 1) indicating their inverse nature.

Frequency response (14a) of the ideal decomposition filter for the time-domain data is a complex function. From the symmetry property of the Fourier transform [10], it follows that the appropriate impulse response has no symmetry, or, in the language of filters, the decomposition filters for the time-domain data belong to so-called *non-linear phase* systems.

In contrast, frequency response (14b) is a pure imaginary function, whereas response (14c) is a real function. This indicates that the decomposition filters for the frequency-domain data are *linear phase systems*.

In Fig. 2(a, b), schematic approximation of ideal frequency response (14b) is shown by the appropriate frequency responses of a discrete-time filter

$$H\left(e^{j\mu}\right) = \sum_n h[n]\exp(-j\mu n \ln q) \quad (15)$$

with odd and even number of coefficients.

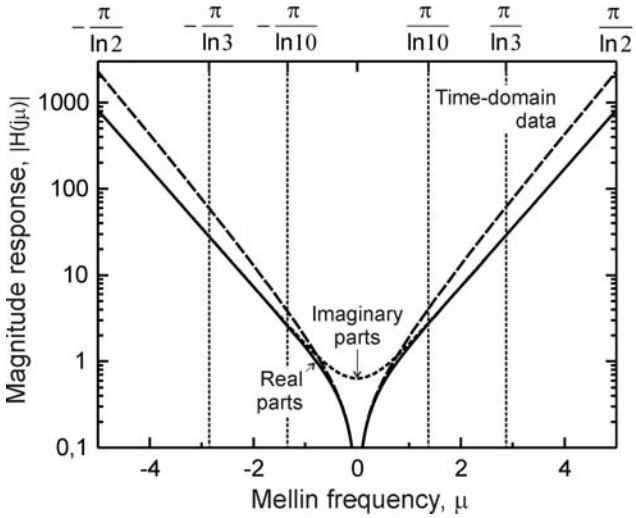

Fig. 1. Magnitude responses of the three ideal decomposition filters. Vertical lines and upper X-axis show the bandwidths corresponding to different progression ratios q

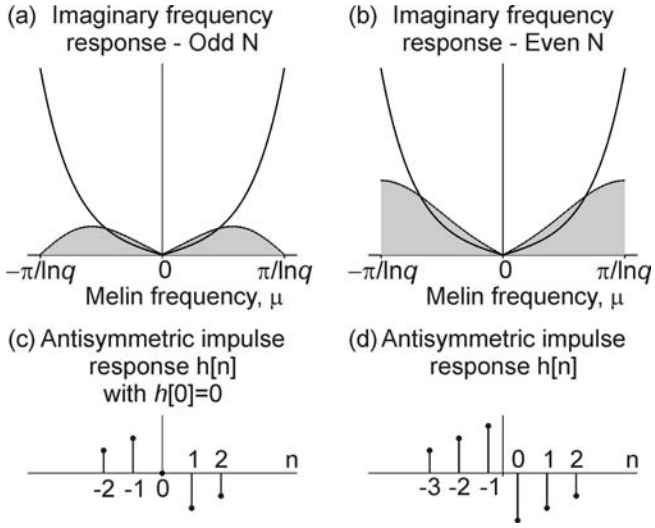

Fig. 2. Schematic approximation of frequency response (14b) with an odd (a) and an even (b) number of coefficients, and examples of the appropriate discrete impulse responses (c) and (d)

In the case of an odd number of coefficients, a decomposition filter represents a *type III linear phase system* [10] having the frequency response, which crosses zero at the ends of bandwidth $\mu = \pm\pi/\ln q$ and at zero frequency (Fig. 2(a)). It has an anti-symmetric impulse response $h[n] = -h[-n]$ with $h[0] = 0$ (Fig. 2(c)). In the case of an even number of coefficients, a decomposition filter represents a *type IV linear phase system* having the frequency response crossing zero at zero frequency and having non-zero values at the ends of the bandwidth $\mu = \pm\pi/\ln q$ (Fig. 2(b)) with an anti-symmetric impulse response $h[n] = -h[-n-1]$ (Fig. 2(d)).

In Fig. 3, the similar plots are shown for the decomposition filters with ideal frequency response (14c) for the imaginary parts. In this case, a filter with an odd number of coefficients represents a *type I linear phase system* with a symmetric

impulse response $h[n]=h[-n]$ (Fig. 3(c)), whereas a filter with an even number of coefficients represents a *type II linear phase system* with a symmetric impulse response $h[n]=-h[-n-1]$ (Fig. 3(d)).

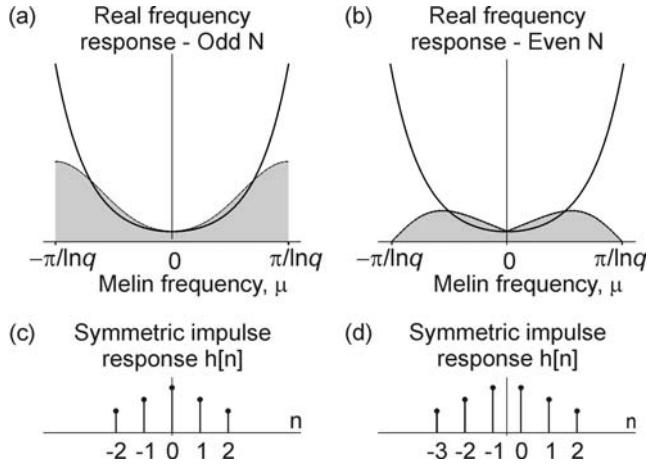

Fig. 3. Schematic approximation of frequency response (14c) with odd (a) and even (b) number of coefficients, and examples of the appropriate discrete impulse responses (c) and (d)

IV. Noise Behavior and Ill-Posedness

For linear systems, random input signals or noise with a Gaussian probability distribution produces output signals that also have a Gaussian probability distribution [10]. Thus, the noise behavior of a decomposition filter as a linear system (on the logarithmic domain) may be described by noise coefficient *S* transforming input noise variance σ_x^2 into the output noise variance σ_y^2

$$\sigma_y^2 = S\sigma_x^2$$

being equal to sum of the square filter coefficients

$$S=\sum_{n=1}^{N} h^2[n]. \tag{16}$$

The Parseval theorem [10] allows determining noise coefficient *S* also through frequency response

$$S=\ln q/(2\pi)\int_{-\pi/\ln q}^{\pi/\ln q}\left|H(.)\right|^2 d\mu, \tag{17}$$

where ideal frequency responses (14a) – (14c) give inherent to the specific decomposition problem theoretical noise coefficients S_{theor}, whereas frequency response (15) of a discrete-time decomposition filter provides actual experimental noise coefficient (16) for the given progression ratio *q*.

As it follows from (17), increasing the sampling rate (decreasing *q*) extends bandwidth [$-\pi/\ln q$, $\pi/\ln q$] of a filter (see Fig. 1), and, consequently, the appropriate area under the magnitude response quoting the value of the noise coefficient. Due to the increasing frequency responses, the theoretical noise coefficient increases with decreasing progression ratio *q* and tends to ∞, when *q* approaches 1 (see curve S_{theor} in Fig. 4). Thus, the ill-posedness of the decomposition manifests as the large noise amplification coefficient coming from the large area under magnitude response, which, in its turn, results from the wide bandwidth. The useful conclusions may be made from the above that the ill-posedness:

(i) may be related and quantitatively characterized by the noise coefficients,

(ii) may be controlled or the decomposition may be regularized by choosing sampling rate, which through establishing the bandwidth of a filter regulates its noise transformation coefficient.

V. Algorithm Design

Algorithm design of a decomposition filter is a complex problem [14], which to the contrary the conventional two-step discrete-time signal processing approach [10] including completely separate (i) signal acquisition step, where the signal is sampled uniformly above its Nyquist rate, and (ii) discrete-time algorithm implementation step, shall actually integrate together three steps: (i) signal acquisition, (ii) regularization and (iii) discrete-time filter design. As a result, filter coefficients shall be obtained for an optimum combination of progression ratio *q* and number of filter coefficients *N* ensuring the needed noise immunity. It should be noted that in practice the available time or frequency ranges of input functions limit the available combinations of *q* and *N*.

To link *q* and *N* with the available input data, a parameter – dynamic range of time or frequency of input signal portion used for computing an output sample (further 'input window range')

$$d_x = u_+ / u_- = q^{N-1} \tag{18}$$

is introduced, which determines the combinations of *q* and *N* allowable for the filter design.

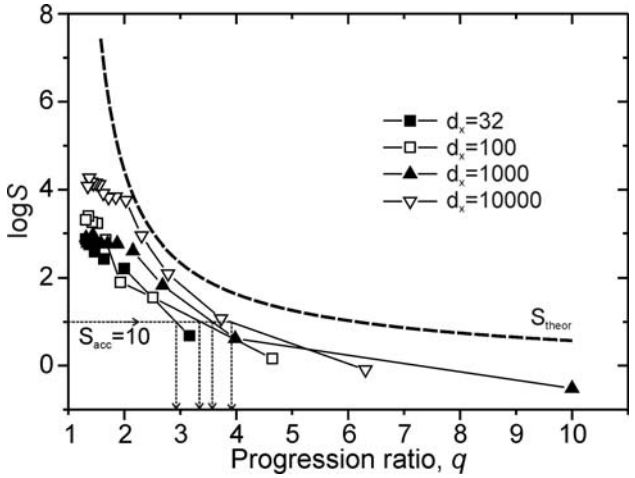

Fig. 4. Theoretical and experimental noise coefficients of the decomposition filters having even number of coefficients for various input window ranges d_x. Vertical arrows show the values of *q* corresponding to an acceptable noise coefficient S_{acc}=10

The proposed algorithm design method [14] is based on designing trial filters for the combinations of q and N allowed by (18) starting with one operating at explicitly large q (low noise coefficient) by subsequent iterative decrease of q and the appropriate increase of N, while the previously fixed acceptably low noise coefficient S_{acc} is achieved.

For the given specification q and N, a filter is designed by the identification method [11] where a pair of theoretical functions interrelated with each other by theoretical deconvolution (7) is used as input and output signals in the filter design. An advantage of the identification method is that it effectively disposes of various secondary effects such as data truncation, rounding-off, etc. and allows designing filters of various types (e.g. with linear and non-linear phase).

VI. Example of a Decomposition Filter

Let assume that a filter with an even number of coefficients having noise coefficient $S < 10$ and employing input window range $d_x \le 500$ must be designed for decomposing the frequency-domain multi-component signal with mono-components (4d).

In Fig.4, the theoretical and experimental noise coefficients are shown as a function of progression ratio q for various input window ranges d_x. Here, the plots are obtained by testing the filters designed by the identification method [11]. From Fig. 4, it follows that progression ratio must be within interval $q = 2.9 - 3.9$ to ensure noise coefficient $S_{acc} \approx 10$. We choose q = 3.3. Then $N = 6$ according to (18) gives d_x = 391 ($d_x \le 500$). By the identification method, the following coefficients have been obtained [15]:

$$h[6] = \{-0.033296, 0.129207, -1.05880, 1.05880, -0.129207, 0.033296\}.$$

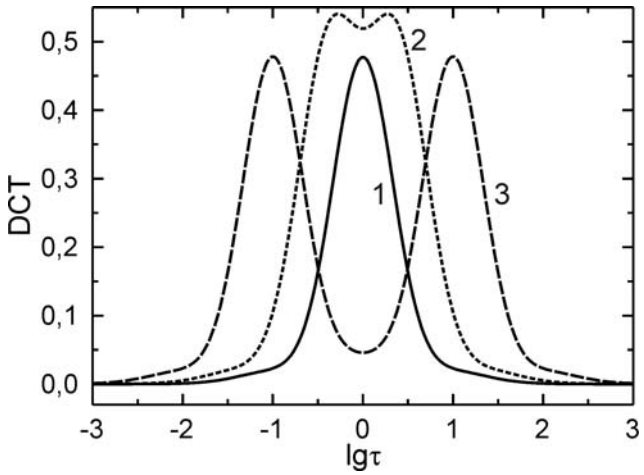

Fig. 5. Recovered DTCs from the noiseless input signals: unity line spectrum at τ = 1 (curve 1); two unity line spectra at τ_1 = 0.42 and τ_2 = 2.37 (curve 2) and at τ_1 = 0.1 and τ_2 = 10 (curve 3)

In Fig. 5, examples of discrete DTCs are shown recovered from the noiseless input data by the designed filter. The recovered DTCs are calculated by algorithm (13c) modified according to (13e) into the form

$$F(\tau) = \sum_{n=-3}^{2} h[n] x(3.3^{-0.5-n} / \tau)$$

with making substitution $\tau = u_0 q^m$. Notice that the designed filter gives DTCs without non-physical oscillations. However, it should be noted that such smoothed spectra are achieved at the expense of decreased resolution; the filter allows separating two spectral lines only, if $\tau_{i+1} / \tau_i < 0.2$ or $\tau_{i+1} / \tau_i > 5$. In general, the proposed decomposition filters are more preferable for recovering continuous DTC [15].

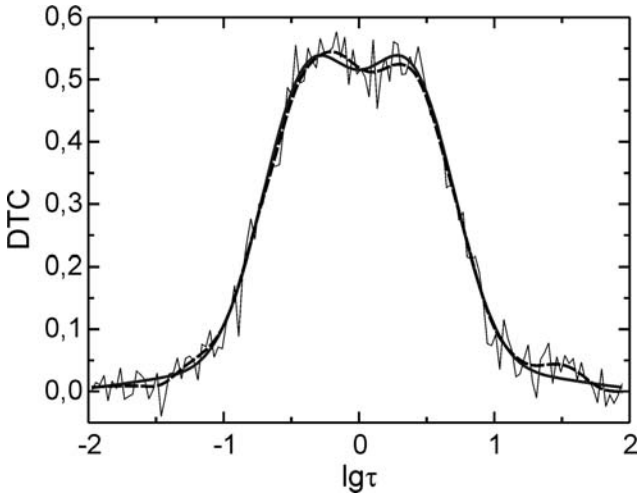

Fig. 6. Recovered DTC for two unity line spectra at τ_1 = 0.42 and τ_2 = 2.37 from the noiseless input signal (fat solid curve) and the noisy input signal (thin solid curve), and noisy DTC smoothed 10 times by (19) (dotted curve)

According to (16) the designed filter has noise coefficient S = 2.28, which means that the noise variance for recovered DTC is amplified 2.28 times or the standard deviation and, consequently, the amplitude of DTC noise is amplified $\sqrt{2.28} = 1.51$ times to compare with that of the input signal.

In Fig. 6, the simulation results are shown for two unity line spectra at $\tau_1 = 0.42$ and $\tau_2 = 2.37$ recovered from the noiseless input signal and from the noisy input signal corrupted by additive random noise

$$x_{noisy}(u_m) = x_{exact}(u_m) + 0.05 \cdot n(m),$$

where $n(m)$ is the pseudorandom sequence within interval [-1,1] with zero mean having the Gaussian probability distribution. The simulation results confirm the above mentioned noise amplification, the recovered DTC indeed represents DTC obtained from the noiseless input signal with additive random noise $\sqrt{S} \cdot 0.05 \cdot n(m) \approx 0.076 \cdot n(m)$. However, DTC smoothing, e.g. by simple 5-point averaging

$$\overline{F}(\tau_m) = \frac{1}{5} \sum_{n=-2}^{2} F(\tau_{m+n}) \qquad (19)$$

allows one to obtain result, which is in rather good agreement

with DTC obtained from the noiseless input data.

VII. Conclusions

FIR filters operating with data equally spaced on a logarithmic scale (geometrically spaced on linear scale) are proposed to use for decomposition of multi-exponential and related signals, such as integrals, derivatives, real and imaginary parts of the Fourier transforms of the real exponentials. The filter algorithms are derived for various time-domain and frequency-domain mono-components. It is shown that the non-linear phase filters have to be used for the time-domain signals, whereas the linear phase filters shall be used for frequency-domain ones. A novel regularization strategy is developed based on filter bandwidth control by choosing the appropriate sampling rate, which allows ensuring the required noise immunity of the algorithms. Algorithm design is suggested integrating together the signal acquisition, the regularization and the discrete-time filter implementation.

References

[1] D. G. Gardner J. C. Gardner, G. Laush, and W. W. Meinke, "Method for analysis of multicomponent exponential decay curves," *J. Chem. Phys.*, vol. 31, no. 4, pp. 978-986, 1959.

[2] T. Schlesinger, "Fit to experimental data with exponential functions using the fast Fourier transform," *Nucl. Instr. Meth.*, vol. 106, no. 3, pp. 503-508, 1973.

[3] F. C. Roesler, and J. R. A. Pearson, "Determination of relaxation spectra from damping measurements," *Proc. Phys. Soc*., vol. 67, no. 412B, pp. 338-347, 1954.

[4] F. C. Roesler, "Some applications of Fourier series in the numerical treatment of linear behaviour," *Proc. Phys. Soc.*, vol. 68, no. 422B, pp. 89-96, 1955.

[5] R. Prost, and R. Goutte, "Linear systems identification by Mellin deconvolution," *Int. J. Control*, vol. 23, no. 4, pp. 713-720, 1976.

[6] R. Prost, and R. Goutte, "Performance of the method of linear systems identifications by Mellin deconvolution," *Int. J. Control*, vol. 25, no. 1, pp. 39-51, 1977.

[7] J. D. Ferry, *Viscoelastic Properties of Polymers*, 3rd ed., New York: J. Wiley and Sons, 1980.

[8] N. G. McCrum, B. E. Read, and G. Wiliams, *Anelastic and Dielectric Effects in Polymer Solids*, London: J. Wiley and Sons, 1967.

[9] A. K. Jonscher, *Dielectric Relaxation in Solids*, London: Chelsea Dielectric, 1983.

[10] A. V. Oppenheim, and R. V. Schafer, *Discrete-Time Signal Processing*, 2nd ed., New Jersey: Prentice-Hall International, 1999.

[11] V. Shtrauss, "Functional conversion of signals in the study of relaxation phenomena", *Signal Processing*, vol. 45, 1995, pp. 293-312.

[12] V. Shtrauss, "Digital signal processing for relaxation data conversion," *J. Non-Crystal. Solids*, vol. 351, 2005, pp. 2911-2916.

[13] V. Shtrauss, "Signal processing in relaxation experiments," *Mech. Comp. Mat.*, vol. 38, 2002, pp. 73-88.

[14] V. Shtrauss, "Sampling and algorithm design for relaxation data conversion," *WSEAS Transactions on Signal Processing*, vol. 2, issue 7, 2006, pp. 984-990.

[15] V. Shtrauss, "Digital estimators of relaxation spectra," *J. Non-Crystal. Solids*, vol. 353, 2007, pp. 4581-4585.

Vairis Shtrauss was born in Sabile, Latvia, in 1946. He was an undergraduate at the Riga Polytechnic Institute (now Riga Technical University). He received the degree of *Cand. Sc. Ing.* in former USSR (*Ph. D.* in Western countries) in the speciality "Polymer Physics and Mechanics" from the Institute of Polymer Mechanics (IMP) of the Latvian Academy of Sciences (LAS) in 1978. In 1993, he received the degree of *Dr. Habil. Sc. Ing.* in the speciality "Instrumentation Engineering" from the Institute of Physical Energy of LAS.

In 1969, he joined IMP, where he was an Engineer and Senior engineer. From 1972 until 1975, he was a Postgraduate Student of IMP. After that he was a Junior Researcher, Researcher and Senior Researcher. From 1993, he is a Principal Researcher, and from 2001 also Head of Laboratory of Non-destructive Testing of IMP of the University of Latvia. His general research interests include information technologies and signal processing for relaxation spectroscopy and material research. He is an author of about 200 scientific publications.

Dr. Shtrauss is a member of the International Dielectric Society, a member of several TC of the Latvian National Standardization institution (Latvian Standard) and an expert and assessor of the Latvian Accreditation Bureau (LATAK).